

Double Lynden-Bell Structure of Low-Energy Quasi-Stationary Distributions in the Hamiltonian Mean Field Model

Eiji Konishi* and Masa-aki Sakagami†

Graduate School of Human and Environment Studies, Kyoto University, Kyoto 606-8501, Japan

(Dated: June 9, 2019)

We study the core-halo structure of low-energy quasi-stationary states in the Hamiltonian mean field model. The core-halo structure results in the superposition of two independent Lynden-Bell distributions. We examine the completeness of the Lynden-Bell relaxation and the relaxation between these two Lynden-Bell distributions.

Introduction.— One of the most interesting feature of long-range systems is the existence of their non-equilibrium and long-lived quasi-stationary state (QSS).[1] The life time of QSS diverges with the number of particle, and QSS temporally separates the Vlasov collisionless regime from the collisional regime of the system. There have been many efforts to reveal the various type structures of QSSs appearing in self-gravitating systems, plasma systems and other simplified models in diverse dimensions.[1, 2] Recently, it has been a great challenge to understand the non-equilibrium core-halo structure in QSSs beyond the paradigmatic Lynden-Bell model of QSSs in such long-range systems.[2, 3]

The Hamiltonian mean field (HMF) model is an accepted toy model of the long-range system.[1, 4] In the one-dimensional HMF model, Pakter and Levin had explained the origin of their proposed uniform core-halo structure of QSSs at low total energies by the parametric resonance of the initial (first one or two periods of) strong oscillation of magnetization.[5] The resonant particles form the high-energy *halo* and, at the same time, rest particles condense into the low-energy dense *core* as a Fermi degeneration like phenomenon due to the Vlasov incompressibility. The resultant distribution is obviously different from the Lynden-Bell equilibrium one[3, 6]. Benetti et al.[7] advanced Pakter and Levin's argument to the global ergodicity breaking and introduced the generalized virial condition (GVC) on the HMF model whose deviation reflects the deviation from the Lynden-Bell equilibrium.

Pakter and Levin proposed the core-halo structure in QSSs in the HMF model as *attachment* of two energy water-bag distributions.[5] In contrast, we investigate the possibility of the core-halo structure in QSSs as a *superposition* of two independent Lynden-Bell energy distributions, that is, the *double Lynden-Bell structure*. The halo part of this structure fits the deviation part from the Lynden-Bell equilibrium in general cases, and to be remarkably noted, this structure conserves the local ergodicity for the core and the halo independently. In this

Letter, at low total energies, we purpose to corroborate this scenario in the HMF model and examine the completeness of relaxation[8, 9] in two kinds: by using the Lynden-Bell entropy and by using the double Lynden-Bell entropy.

The model.— The N -body HMF model treats N -identical interacting particles with unit mass on a circle. Their dynamics is governed by the Hamiltonian

$$H = \sum_{j=1}^N \frac{p_j^2}{2} + \frac{1}{2N} \sum_{j,k=1}^N [1 - \cos(\theta_j - \theta_k)] , \quad (1)$$

where angle θ_j is the orientation of the j -th particle and p_j is its conjugate momentum.[1, 4] Throughout this Letter, both of the particle number N and the simulation time t are assumed to be 10^4 . We choose the phase constant of the one-body mean-field potential as $\Phi(\theta, M) = 1 + M \cos \theta$. M denotes the magnetization of the system. The one-particle energy function is $\varepsilon(\theta, p, M) = p^2/2 + \Phi(\theta, M)$. The self-consistency condition, regarding this mean-field methods, on energy distribution $f(\varepsilon)$ is

$$M = -\frac{1}{N} \int d\theta dp \cos \theta f(\varepsilon(\theta, p, M)) . \quad (2)$$

Now, we explain the formation machinery of the core-halo structure of the HMF system at low total energy. By the trigger, which creates the chemical potential gap, by the parametric resonance of the system with the initial strong oscillation of the magnetization, the core-halo structure starts forming. After dynamical processes undergone by particle and energy exchanges between the core and the halo, the QSS distribution relaxes to the *stationary* superposition of two components, that is, the core and the halo. (Due to the long-range nature, the potential $\Phi(\theta, M)$ is common between the core and halo distributions.) We denote the core and halo distributions by f_c and f_h . (We shall denote the normalization of norm by the factor $1/N$ by the hat.) The dynamical relaxation between the core and the halo

$$df_a/dt \rightarrow 0 , \quad a = c, h \quad (3)$$

plays the same role of the Vlasov fluid property of incompressibility for each component $a = c, h$. This leads to

*Corresponding Author.

that the phase-space density η_a of each f_a freezes under $\eta = \eta_c + \eta_h$. When phase-mixing for the both components has completed, $f(\theta, p)$ becomes a function of ε only, and due to Eq.(3), $\partial f_a(\varepsilon)/\partial t = 0$ holds, thus the total mass N_a of f_a freezes. More on it, since in QSS the magnetization stabilizes, the total energy E_a of f_a also freezes. Consequently, the core-halo formation is completed.

Based on this machinery, we derive the collisionless entropy and the core-halo QSS distribution, by following the manner to discuss the collisionless relaxation as done by Lynden-Bell.[3] In this manner, the phase space is divided by macro-cells, i.e., assemblies of micro-cells. Micro-cells are occupied by incompressible Vlasov elements. The core and halo phase-space distribution functions, that are coarse-grained by the unit of macro-cell, are defined by

$$f_c(\theta_i, p_i) = f_{c,i} = \frac{\eta m_i \omega}{\nu \omega} = \frac{\eta_c m_i}{\nu_c}, \quad \eta_c = \frac{\eta}{\nu} \nu_c, \quad (4)$$

$$f_h(\theta_i, p_i) = f_{h,i} = \frac{\eta n_i \omega}{\nu \omega} = \frac{\eta_h n_i}{\nu_h}, \quad \eta_h = \frac{\eta}{\nu} \nu_h, \quad (5)$$

where i labels macro-cells ($i = 1, \dots, p$), m_i and n_i are numbers of Vlasov elements occupying i -th macro-cell, ν is the number of micro-cells in each macro-cell, and ω is the area of each micro-cell. Due to the machinery explained above, the following partitions are fixed:

$$N = N_c + N_h, \quad E = E_c + E_h, \quad \nu = \nu_c + \nu_h. \quad (6)$$

The third partition is kept for the ratios in the continuum limit $\nu \rightarrow 0$. The total partition number of the configurations of the Vlasov elements in the phase space is

$$W = W_{mix} W_{lb}^{(c)} W_{lb}^{(h)}, \quad (7)$$

$$W_{mix} = \frac{N!}{N_c! N_h!}, \quad (8)$$

$$W_{lb}^{(c)} = \frac{N_c!}{\prod_{i=1}^p m_i!} \prod_{i=1}^p \frac{\nu_c!}{(\nu_c - m_i)!}, \quad (9)$$

$$W_{lb}^{(h)} = \frac{N_h!}{\prod_{i=1}^p n_i!} \prod_{i=1}^p \frac{\nu_h!}{(\nu_h - n_i)!}, \quad (10)$$

where W_{mix} is the partition number of mixing the core and the halo and $W_{lb}^{(a)}$ is the Lynden-Bell partition number for the core and the halo. Using Eqs.(4) and (5), the total partition number W is reexpressed as a functional of coarse-grained distributions $f_{c,i}$ and $f_{h,i}$. Maximization procedure of the micro-canonical entropy by these is[11]

$$\delta_{f_{c,i}} \ln W = 0, \quad \delta_{f_{h,i}} \ln W = 0 \quad (11)$$

under the constraints Eq.(6). We introduce two kind Lagrange multipliers α_a and β_a for fixed particle number N_a and energy E_a , for $a = c, h$, respectively. Under the continuum limit ($\nu \rightarrow 0$), the total entropy reduces to

$$S = S^{(c)} + S^{(h)}, \quad (12)$$

where each $S^{(a)}$ is the Lynden-Bell entropy[3]

$$S^{(a)} = - \int d\theta dp \left(\frac{f_a}{\eta_a} \ln \frac{f_a}{\eta_a} + \left(1 - \frac{f_a}{\eta_a} \right) \ln \left(1 - \frac{f_a}{\eta_a} \right) \right) \quad (13)$$

for $a = c, h$. The maximization solution of Eq.(12) is the double Lynden-Bell distribution

$$f(\theta, p) = \sum_{a=c,h} \frac{\eta_a}{\exp(\beta_a(\varepsilon(\theta, p, M) - \mu_a)) + 1}, \quad (14)$$

where $\mu_a = -\alpha_a/\beta_a$ is the chemical potential of the core and the halo. Here, the readers may think that since the partition number W consists of product Eq.(7), the distribution function Eq.(14) would also consist of product. However, the fine grains of distribution functions f_c and f_h do not share any same micro-cell. Thus, f is a superposition, i.e., $f = f_c + f_h$.

Simulation results and discussions.— In the N -body simulation performed in this Letter, the initial phase-space distribution function $\hat{f}_0(\theta, p)$ is the uniform water-bag type distribution over a rectangle $[-\theta_0, \theta_0] \times [-p_0, p_0]$, namely

$$\hat{f}_0(\theta, p) = \hat{\eta} \Theta(\theta_0 - |\theta|) \Theta(p_0 - |p|), \quad (15)$$

where Θ is the Heaviside unit one-step function. The parameters θ_0 and p_0 of Eq.(15) satisfy the relations $\sin \theta_0/\theta_0 = M_0$, $p_0 = \sqrt{6\hat{E} - 3(1 - M_0^2)}$, and $\hat{\eta} = 1/(4\theta_0 p_0)$ for the initial magnetization M_0 and the energy per particle \hat{E} . By these relations, when we fix $\hat{\eta}$, we can produce \hat{E} from M_0 . In order to take the advantage of the Vlasov incompressibility, that is, the dynamical conservation of $\hat{\eta}$, we classify simulation data by the common $\hat{\eta}$. In this Letter, we adopt 0.15.

FIG. 1: This figure shows $\hat{\eta} = 0.15$ configuration of four data $M_0 = 0.53, M_{\min}, 0.72, 0.78$ on (M_0, \hat{E}) plane to be used in Figs.3 and 4. Here, $M_{\min} \sim 0.6556$ is the magnetization of the initial water-bag distribution Eq.(15) at the minimum \hat{E} . The blue and red curves represent the initial water-bag states and the energy per particle of the Vlasov stationary state $f_{\varepsilon F}$ for $\eta = 1500$, respectively.

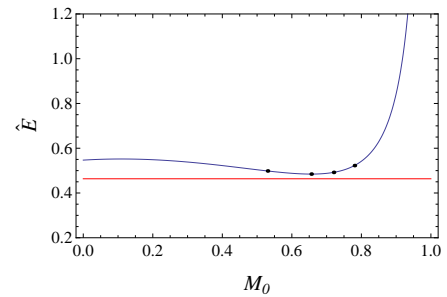
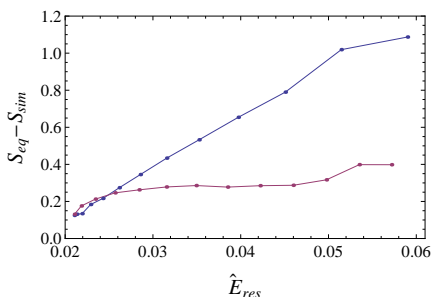


Figure 1 shows that $M_0 = M_{\min}$ gives the global minimum of the function $E(M_0)$ and in the neighbor of it, this function is convex. This fact stands also in other

cases of $\hat{\eta}$. Thus, it is a natural way to cast some properties of the system in its total energy E . According to this line, we introduce the residual total energy E_{res} of the total energy E of the system against the total energy E_{ε_F} (the red line in Fig.1) of the Vlasov stationary state $f_{\varepsilon_F}(\varepsilon) = \eta\Theta(\varepsilon_F - \varepsilon)$ for $\eta = 1500$ (i.e., $E_{\text{res}} = E - E_{\varepsilon_F}$). [12] To clarify the meanings of E_{res} , we consider dynamics of the system on the phase space. When dynamics start from f_0 , its center f_{ε_F} is Vlasov stationary, and there is the total energy gap $E_{\text{res}} > 0$ between them. So, by using E_{res} the system creates the halo of high-energy particles in the outer site, then, the inner part approaches this Vlasov stationary state due to the energy conservation law. Thus, E_{res} measures the degree of the creation of the high-energy tail of the halo, which deviates the system from the Lynden-Bell equilibrium. Namely, we argue that E_{res} is a measure of the deviation of the system from the Lynden-Bell equilibrium. In the cases of $M_0 \leq M_{\text{min}}$, the inscribed and the circumscribed Vlasov stationary distributions to the initial distributions Eq.(15) are close to each other. So, in these cases, the validity of this argument weakens. In Fig.2, we illustrate this argument as the almost monotonous correspondences between the residual total energy and the residue of the Lynden-Bell entropy of the Lynden-Bell equilibrium against that of the system. As easily con-

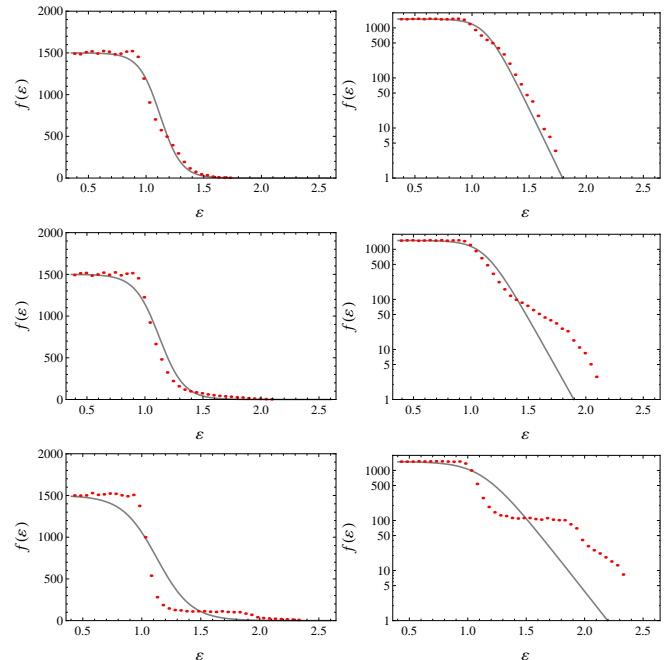
FIG. 2: This figure shows the residue of the Lynden-Bell entropy of the Lynden-Bell equilibrium S_{eq} for given E and $\eta = 1500$ against that of the simulation result S_{sim} as the function of the residual energy per particle \hat{E}_{res} . Blue and purple thirteen plotted dots represent the cases of $M_0 = 0.66 \sim 0.78$ (with 0.01 increments) and $M_0 = 0.41 \sim 0.65$ (with 0.02 increments) using 10 run averages, respectively.



firmed, the minimization condition on the residual total energy $(\partial E_{\text{res}}/\partial M_0)_\eta = 0$ matches to the GVC for the HMF model discussed in Ref.[7]. So, this argument is our advantage to the GVC formulation.

As illustrated in Fig.3, for higher residual total energy E_{res} read from Fig.1, the high-energy tail of the simulation resultant $f(\varepsilon)$ grows more. This high-energy tail makes the simulation resultant $f(\varepsilon)$ to deviate from the Lynden-Bell equilibrium. In the double Lynden-Bell scenario, we argue that this deviation part is fitted by the halo part of the distribution, f_h . As the illustration of this argument, in Fig.4 we show the *theoretical*

FIG. 3: These figures show the deviation of the simulation resultant $f(\varepsilon)$ (red dots) averaged over 20 runs from the single Lynden-Bell equilibrium (gray curve) in the cases of $M_0 = M_{\text{min}}, 0.72, 0.78$ (from up to down).



semi-predictions of the cases with three initial magnetizations $M_0 = 0.53, M_{\text{min}}$ and 0.78 by double Lynden-Bell distributions. (Note that a double Lynden-Bell distribution has seven degrees of freedom. In Fig.4, by adjusting three parameters of it by hand, we solve the four conditions, that is, three conservation laws on mass, energy and phase-space density, and the self-consistency condition Eq.(2) and derive the double Lynden-Bell distributions. So, Fig.4 is not just a fitting but a theoretical result.) The adjusted three parameters in Fig.4 include the Lynden-Bell entropy. Owing to setting the Lynden-Bell entropy to be lower than that of the Lynden-Bell equilibrium, we accurately reproduce the N -body simulation results. These accurate reproductions corroborate the double Lynden-Bell scenario.

As a basic quest, it is worth to examine whether or not the simulation resultant QSSs complete the relaxation between the core and halo Lynden-Bell distributions, whose criterion is weaker than that of the Lynden-Bell relaxation. The relaxation criterion to be considered is cast in the *on-shell* maximization of the double Lynden-Bell entropy Eq.(12):

$$\frac{\partial S}{\partial N_c} \Big/ \frac{\partial M_s}{\partial N_c} = \frac{\partial S}{\partial E_c} \Big/ \frac{\partial M_s}{\partial E_c} = \frac{\partial S}{\partial \eta_c} \Big/ \frac{\partial M_s}{\partial \eta_c}, \quad (16)$$

where the stationary magnetization M_s is fixed by hand. The case $M_0 = 0.72$ fulfils this criterion for $M_s = 0.6345$, which is within the oscillation range of the stationary magnetization (see Fig.5). However, in other cases of M_0 ,

FIG. 4: These figures show $M_0 = 0.53$, $M_{\min}, 0.78$ (from up to down) double Lynden-Bell theoretical semi-predictions of simulation resultant $f(\varepsilon)$ (red dots) averaged over 20 runs. Green and cyan curves represent full and the halo part of double Lynden-Bell distribution, respectively, under the three conservation laws and the self-consistency condition Eq.(2) and by adjusting values of the Lynden-Bell entropy, stationary magnetization M_s and η_c by hand. Gray-dashed curve represents the Lynden-Bell equilibrium for given E and $\eta = 1500$.

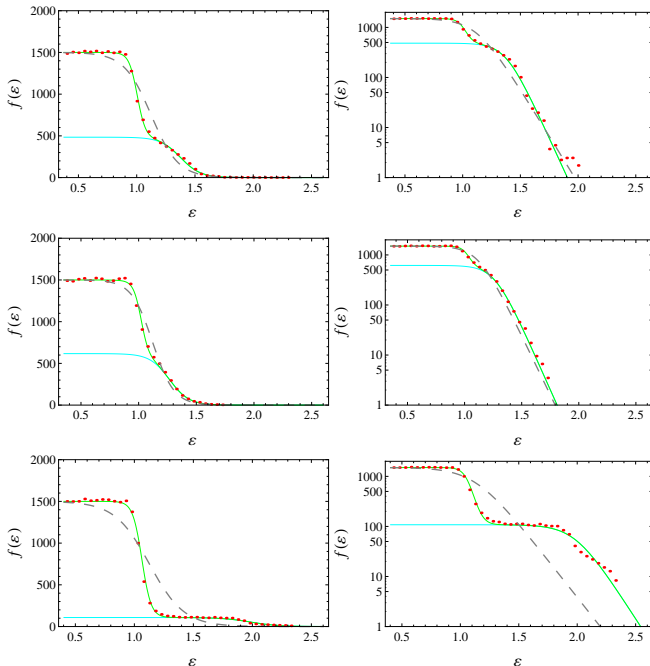
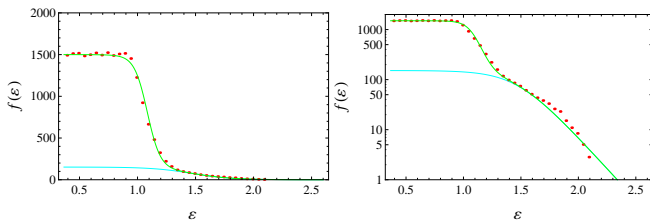


FIG. 5: These figures show $M_0 = 0.72$ theoretical result of $f(\varepsilon)$ by solving the on-shell entropy maximization condition for $M_s = 0.6345$ (its full and the halo part are drawn by green and cyan curves, respectively), and the simulation resultant $f(\varepsilon)$ averaged over 20 runs (red dots).



the simulation results do not fulfil the on-shell entropy maximization criterion and are regarded in the case of incomplete relaxation of Eq.(12).

Summary and outlook.— In the HMF model, we have systematically studied the core-halo structure of the QSSs for the initial rectangle water-bag distributions

with $\hat{\eta} = 0.15$ and corroborated the double Lynden-Bell scenario at low total energies. More on this result, we examined the completeness of relaxation by using two entropies. By using the Lynden-Bell entropy, we found that the systems being considered do not reach at the equilibrium and for higher total energy the incompleteness degree grows more. By using the double Lynden-Bell entropy, in the case of $M_0 = 0.72$, the system completes the relaxation; however other cases of M_0 do not.

We suggest two open issues. First issue is on finding a measure of deviation from the complete relaxation between the core and halo Lynden-Bell distributions. Second, it is a significant issue to determine the total energy limit of application of the double Lynden-Bell scenario and extend our ideas to the systems at high total energies reported in Ref.[10].

We are grateful to T. Tashiro and T. Tatekawa for valuable discussions, especially to T. Tatekawa for providing us the Fortran code for the HMF simulation.

† konishi.eiji.27c@st.kyoto-u.ac.jp;
sakagami.masaaki.6x@kyoto-u.ac.jp

- [1] A. Campa, T. Dauxois and S. Ruffo, Phys. Rep. 480, 57 (2009) [arXiv:0907.0323].
- [2] Y. Levin, R. Pakter, F. B. Rizzato, T. N. Teles and F. P. C. Benetti, Phys. Rep. 535, 1 (2014) [arXiv:1310.1078].
- [3] D. Lynden-Bell, Mon. Not. R. astr. Soc. 136, 101 (1967).
- [4] M. Antoni and S. Ruffo, Phys. Rev. E 52, 2361 (1995).
- [5] R. Pakter and Y. Levin, Phys. Rev. Lett. 106, 200603 (2011) [arXiv:1012.0035].
- [6] A. Antoniazzi, D. Fanelli, J. Barre, P. H. Chavanis, T. Dauxois and S. Ruffo, Phys. Rev. E, 75, 011112 (2007) [arXiv:cond-mat/0603813].
- [7] F. P. C. Benetti, T. N. Teles, R. Pakter and Y. Levin, Phys. Rev. Lett. 108, 140601 (2012) [arXiv:1202.1810].
- [8] P. H. Chavanis, Physica. A. 365, 102 (2006) [arXiv:cond-mat/0509726].
- [9] P. H. Chavanis, in: N. Antonic et al. (Eds.) *Multiscale Problems in Science and Technology*, (Springer-Verlag, Berlin Heidelberg 2002).
- [10] A. Campa and P. H. Chavanis, Eur. Phys. J. B. 86, 170 (2013) [arXiv:1210.4082].
- [11] We omit the details of the calculations in the following few sentences, since these are parallel to those in the single Lynden-Bell case[3].
- [12] In this context, the Vlasov stationary state f_{ε_F} contains three parameters, that is, the Fermi energy ε_F , the magnetization and the total energy E_{ε_F} . These are determined by the two conservation laws and the self-consistency condition Eq.(2).